Maker fringes revisited: second-harmonic generation from birefringent or absorbing materials

Warren N. Herman

Naval Air Warfare Center, Aircraft Division, Warminster, Pennsylvania 18974

L. Michael Hayden

Department of Physics, University of Maryland Baltimore County, Baltimore, Maryland 21228

Received June 23, 1994

We present a new formulation of Maker fringes in parallel-surface films, using self-consistent boundary conditions for reflections and allowing for any degree of refractive-index dispersion. This treatment of the second-harmonic reflections and dispersion, unlike a number of previous derivations, leads correctly to the expected form for the effective second-harmonic d coefficients. Complete expressions with physically meaningful factors are given for the generated second-harmonic power for either absorbing or birefringent films including reflections for the case of no pump depletion. A comparison with the isotropic approximation is given, and practical considerations in the use of these expressions for the fitting of experimental data are discussed.

1. INTRODUCTION

Since 1970 the determination of the nonlinear optical (NLO) coefficients d_{ij} ($i = 1–3$, $j = 1–6$) associated with second-harmonic generation (SHG) has been performed almost exclusively by the Maker fringe technique[1] as described in detail by Jerphagnon and Kurtz (hereafter, JK).[2] Over the years this technique has been applied to inorganic and organic crystals and organic polymers. However, some of the original assumptions made in the derivations by JK, although they were applicable to the transparent crystals of the day, are not uniformly applicable to all material classes currently under investigation. Also, the theory presented by JK did not consider absorbing materials or the general case of anisotropic media. Many of the second-order NLO organic materials under investigation today, such as liquid crystals, Langmuir–Blodgett films, poled polymers, and organic crystals, are absorbing at the wavelength of the typical SHG experiment and exhibit a fair degree of anisotropy. Unfortunately, during the past 24 years the results of JK were applied, by many workers, to systems that were either anisotropic or absorbing, resulting in errors in the determination of d_{ij}.

In solving the boundary value problem for SHG, JK used approximate boundary conditions for the second-harmonic (SH) waves by ignoring the SH wave reflected from the second interface in the boundary conditions at the first interface and assumed, in portions of their calculations, that the nonlinear material had the same index of refraction at the fundamental frequency ω as it had at the second-harmonic frequency 2ω. As a result, their expression for $p(\theta)$, the angular projection factor for the nonlinearity, is nonintuitive and difficult to calculate in general. Furthermore, it is incorrect for materials for which there is dispersion. These problems are not widely realized in the literature and have continued to propagate, even recently.[3–5] Some authors have realized the problem with $p(\theta)$ and have replaced it in the theory of JK, *ad hoc*, with the correct term.[6] As a result, a combination of the JK theory with an *ad hoc* correction for the projection factor is sometimes used to analyze SHG experiments.

Ignoring reflections, expressions for the sum-frequency fields generated by an isotropic transparent nonlinear parallel slab were given three decades ago by Bloembergen and Pershan.[7] Subsequently to JK, Chemla and Kupecek[8] obtained Poynting vectors for nonlinear wedges in air for anisotropic nonabsorbing materials with 32-point symmetry and for absorbing isotropic materials but, like JK, considered the boundary conditions for the input and output faces of the nonlinear material separately. More recently Okamoto *et al.*[3] obtained expressions for Maker fringes in anisotropic parallel slabs with $C_{\infty v}$ space symmetry, but, again, they used the JK boundary-condition approach, leading to complicated expressions that are not only difficult to interpret physically but also incorrect if reflections are kept and no assumptions are made about the dispersion.

In this paper we provide a new derivation of the Maker fringes, using complete boundary conditions for the SH waves. We also provide a general solution for birefringent media and a separate solution for materials with nonzero absorption of the fundamental and SH waves. This study is intended to provide a general framework for analyzing SHG experiments by use of the Maker fringe technique. Our theory, which includes the reflections of the SH wave in the nonlinear material, is also an extension of an earlier work that neglected those reflections.[9] The new theory predicts the same results as JK for transparent, isotropic materials but exhibits significant differences for materials with nonzero dispersion. These differences have implications for experimentalists investigating the order in poled polymers by measuring the

0740-3224/95/030416-12$06.00

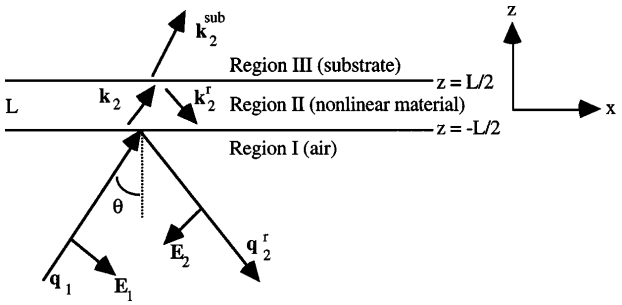

Fig. 1. Three-layer slab geometry for SHG that is due to a nonlinear layer in region II with the origin at the center of the nonlinear film.

ratio d_{31}/d_{33}. We also show that the effect of neglecting the birefringence in the analysis of Maker fringe data can result in large errors in the determination of d_{ij}.

2. THEORY

In this section we present our general approach to the boundary-value problem for SHG. A detailed exposition is given in the appendixes. For simplicity we consider the isotropic case with no absorption first. Briefly, we show how including reflections of the SH wave makes the result less ambiguous than JK do and simpler to use in practice. We agree with the arguments concerning Gaussian beams and multiple reflection of the fundamental beam given by JK and will not repeat them. The major difference between the two approaches is that JK neglected to consider the amplitude at the input boundary of the SH wave reflected from the second interface and we do not.

A. Isotropic Case

As the measurement of d_{ij} of a thin nonlinear film usually requires that the film be supported upon a substrate, we consider the three-layer system as shown in Fig. 1. We assume that an electromagnetic wave of frequency ω is incident upon the structure from the bottom at an angle θ (the x–z plane is the plane of incidence). For a frequency $m\omega$, the nonlinear layer of thickness L has an index n_m and the substrate has an index n_{ms}. For free-standing films or crystal plates, setting the substrate index n_{2s} equal to 1 will suffice.

If we write the electric field of the incident fundamental wave as

$$\mathbf{E}_{1v} = \hat{\mathbf{e}}_v E_1 \exp[i(\mathbf{q}_1 \cdot \mathbf{r} - \omega t)], \tag{1}$$

with $\hat{\mathbf{e}}_v = (0, 1, 0)$ or $(\cos\theta, 0, -\sin\theta)$ for $v = s$ or p, respectively, and $\mathbf{q}_1 = (\omega/c)(\sin\theta, 0, \cos\theta)$, then, for a p-polarized input, the SH fields in the three regions shown in Fig. 1 are given by

$$\begin{aligned}
\text{Region I:}\quad \mathbf{E}_2 &= R\hat{\mathbf{e}}_p^r \exp\{i\mathbf{q}_2^r \cdot [\mathbf{r} + (L/2)\hat{\mathbf{z}}]\},\\
\mathbf{H}_2 &= -(ic/2\omega)\nabla \times \mathbf{E}\\
&= R\hat{\mathbf{e}}_s^r \exp\{i\mathbf{q}_2^r \cdot [\mathbf{r} + (L/2)\hat{\mathbf{z}}]\},
\end{aligned} \tag{2}$$

$$\begin{aligned}
\text{Region II:}\quad \mathbf{E}_2 &= \mathbf{e}_b \exp(i2\mathbf{k}_1 \cdot \mathbf{r}) + A\hat{\mathbf{e}}_{2p} \exp(i\mathbf{k}_2 \cdot \mathbf{r})\\
&\quad + B\hat{\mathbf{e}}_{2p}^r \exp(i\mathbf{k}_2^r \cdot \mathbf{r}),\\
\mathbf{H}_2 &= \mathbf{h}_b \exp(i2\mathbf{k}_1 \cdot \mathbf{r}) + n_2 A\hat{\mathbf{e}}_{2s}\\
&\quad \times \exp(i\mathbf{k}_2 \cdot \mathbf{r})\\
&\quad + n_2 B\hat{\mathbf{e}}_{2s}^r \exp(i\mathbf{k}_2^r \cdot \mathbf{r}),
\end{aligned} \tag{3}$$

$$\begin{aligned}
\text{Region III:}\quad \mathbf{E}_2 &= T\hat{\mathbf{e}}_{2p}^{sub} \exp\left[i\mathbf{k}_2^{sub} \cdot \left(\mathbf{r} - \frac{L}{2}\hat{\mathbf{z}} \right) \right],\\
\mathbf{H}_2 &= n_{2s} T\hat{\mathbf{e}}_{2s}^{sub}\\
&\quad \times \exp\left[i\mathbf{k}_2^{sub} \cdot \left(\mathbf{r} - \frac{L}{2}\hat{\mathbf{z}} \right) \right],
\end{aligned} \tag{4}$$

where $\hat{\mathbf{e}}_s^r = (0, 1, 0)$ or $\hat{\mathbf{e}}_p^r = (-\cos\theta, 0, -\sin\theta)$ is the polarization unit vector for the reflected SH field in air. A and B are the complex amplitudes for the forward and backward SH free waves in the nonlinear medium, respectively, and T and R are the corresponding SH amplitudes in the substrate and air, respectively. The polarization unit vectors for the forward and backward SH waves in the nonlinear medium are $\hat{\mathbf{e}}_{2s} = (0, 1, 0)$ or $\hat{\mathbf{e}}_{2p} = (c_2, 0, -s_2)$ and $\hat{\mathbf{e}}_{2s}^r = (0, 1, 0)$ or $\hat{\mathbf{e}}_{2p}^r = (-c_2, 0, -s_2)$, respectively. For the substrate, $\hat{\mathbf{e}}_{2s}^{sub} = (0, 1, 0)$ and $\hat{\mathbf{e}}_{2p}^{sub} = (c_{2s}, 0, -s_{2s})$. The wave vectors are (outside the nonlinear slab) $\mathbf{q}_2^r = (2\omega/c)(\sin\theta, 0, -\cos\theta)$, (inside the slab) $\mathbf{k}_m = (m\omega n_m/c)(s_m, 0, c_m)$ and $\mathbf{k}_m^r = (m\omega n_m/c)(s_m, 0, -c_m)$, and (in the substrate) $\mathbf{k}_2^{sub} = (2\omega n_{2s}/c)(s_{2s}, 0, c_{2s})$, where $s_m = (1/n_m)\sin\theta$ and $c_m = \sqrt{1 - s_m^2}$. The bound waves are given by

$$\begin{aligned}
\mathbf{e}_b &= \frac{4\pi}{n_1^2 - n_2^2}\left[\mathbf{P}^{NL} - \frac{\mathbf{k}_b(\mathbf{k}_b \cdot \mathbf{P}^{NL})}{|\mathbf{k}_2|^2} \right], \qquad \mathbf{k}_b = 2\mathbf{k}_1,\\
\mathbf{h}_b &= n_1\hat{\mathbf{k}}_1 \times \mathbf{e}_b,\\
\mathbf{P}^{NL} &\equiv |E_1|^2 \vec{\mathbf{d}} : \hat{\mathbf{e}}_1\hat{\mathbf{e}}_1.
\end{aligned} \tag{5}$$

In matching the tangential components of the fields between regions I and II, JK neglect the third terms on the right-hand sides of Eqs. (3). They justify this approximation by assuming that the reflected free wave is small. Because they do so, their solution for the transmitted SH power contains a small term that does not oscillate (which they neglect) and nonstandard Fresnel transmission factors. Furthermore, their projection factor $p(\theta)$ is incorrect because they obtain it by assuming that $n_1 \approx n_2$. Keeping those terms, however, is not difficult and results in an expression that includes the effects of reflection of the SH wave in the nonlinear medium and the correct, general expression for the projection factor $d_{\text{eff}} = \hat{\mathbf{e}}_2 \cdot \vec{\mathbf{d}} : \hat{\mathbf{e}}_1\hat{\mathbf{e}}_1$. As derived in Appendix A, the transmitted SH power from a nonlinear isotropic slab in the geometry depicted in Fig. 1, including reflections of the SH and any degree of dispersion, is then

$$P_{2\omega}^{(\gamma\to p)} = \frac{128\pi^3}{cA}\,\frac{[t_{\text{af}}^{(1\gamma)}]^4[t_{\text{fs}}^{(2p)}]^2[t_{\text{sa}}^{(2p)}]^2}{n_2^2 c_2^2}\,P_\omega^2\left(\frac{2\pi L}{\lambda}\right)^2 d_{\text{eff}}^2\,\frac{\left(\dfrac{\sin^2\Psi}{\Psi^2} + [r_{\text{af}}^{(2p)}]^2R^2\dfrac{\sin^2\Phi}{\Phi^2} - 2r_{\text{af}}^{(2p)}R\dfrac{\sin\Psi}{\Psi}\dfrac{\sin\Phi}{\Phi}\cos 2\phi_2\right)}{(1 + [r_{\text{af}}^{(2p)}r_{\text{fs}}^{(2p)}]^2 + 2r_{\text{af}}^{(2p)}r_{\text{fs}}^{(2p)}\cos 4\phi_2)}, \tag{6}$$

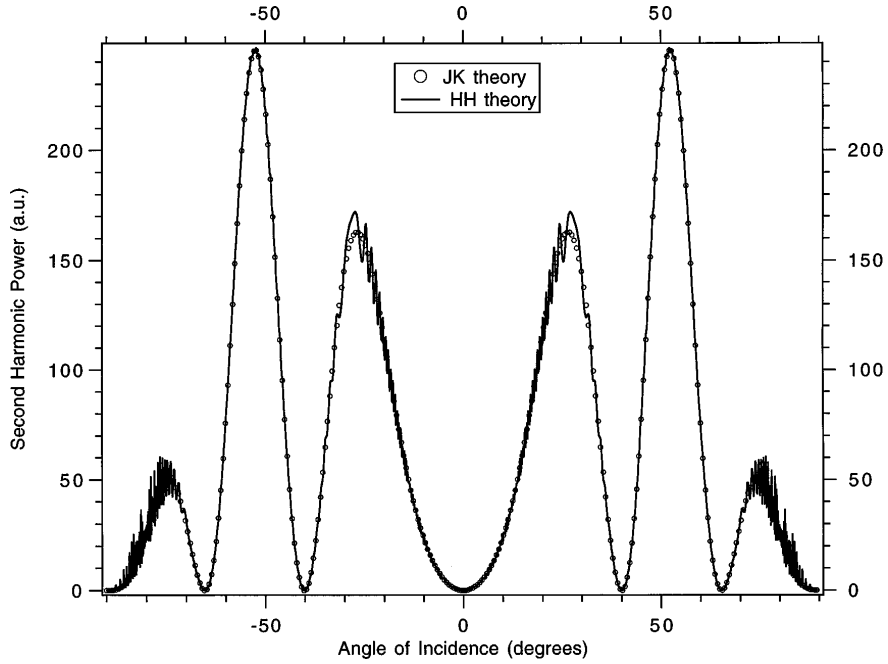

Fig. 2. Maker fringe pattern predicted by JK and HH for a 300-μm-thick piece of X-cut quartz. Rotation is about the z axis.

where the t's and the r's are standard Fresnel transmission and reflection coefficients, respectively, at the air–film, film–substrate, and substrate–air interfaces for the appropriate polarizations and frequencies and where $R = d_{\text{eff}}{}^{r}/d_{\text{eff}}$, $\Psi = (2\pi L/\lambda)(n_1c_1 - n_2c_2)$, $\Phi = (2\pi L/\lambda)(n_1c_1 + n_2c_2)$, and $\phi_2 = (2\pi L/\lambda)(n_2c_2)$. A comparison of the Maker fringe pattern for X-cut quartz predicted by JK and the current (hereafter the HH) method given by Eq. (6) is shown in Fig. 2. The high-frequency oscillations on the HH curve are the result of the reflections of the SH wave in the nonlinear medium. The magnitude of the oscillations is related to the index difference between the nonlinear medium and regions I and III. Figure 2 supports the assertion of JK that the effect of reflections is small. In addition, carefully mapping out the high-frequency oscillations requires an angular resolution far beyond that which is normally attempted.

In terms of the ability to measure d_{ij} accurately, we find that the difference between coefficients determined by considering reflections and neglecting them (<2%) is smaller than the typical experimental error in those measurements (≈10–20%). Because of the small difference predicted in the calculated d_{ij} we will henceforth neglect the reflections by setting $r_{\text{af}}^{(2p)} \approx 0$ in Eq. (6). This action is different from the method used by JK to neglect reflections. JK's approximation of no reflections in the boundary conditions results in the necessity later to assume no dispersion ($n_1 \approx n_2$) and incident angles $\theta_i \leq \pi/4$ in order to reduce the complexity of their result [see Eqs. (A36) and (A38) of JK].

The consequences of these assumptions can be significant for materials with even modest dispersion. Figure 3 shows the effect of dispersion on the measured d_{ij} in a material with $C_{\infty v}$ symmetry. For Fig. 3 we calculated the curves for the d_{33} ratios assuming that $d_{33} = 3d_{31}$. In practice, however, one usually measures d_{31} first and then uses that value in the calculation for d_{33}. This procedure is followed when one is trying to determine the order parameter in a poled polymer achieved by means of electric-field poling. By taking the ratios of the $s \rightarrow p$ and $p \rightarrow p$ transmitted SH powers from the theories of JK and HH, and assuming that $d_{31} = d_{15}$ (Kleinman symmetry), we have derived the following relation:

$$\left(\frac{d_{31}}{d_{33}}\right)_{\text{JK}} = \left[\frac{2c_1(n_2c_2 - n_1c_1)}{n_1{s_1}^2} + \left(\frac{d_{33}}{d_{31}}\right)_{\text{HH}}\right]^{-1}. \quad (7)$$

Figure 4 shows that, as the dispersion increases, the ratio of d_{31}/d_{33} calculated by the JK method decreases. Because the standard rigid-gas model[10] describing the electric-field-induced orientation of dipoles predicts that $d_{31}/d_{33} = 1/3$ for low poling fields and ratios smaller than 1/3 for high poling fields, measured SHG ratios of $d_{31}/d_{33} < 1/3$ are generally attributed to more order. In these cases, however, our results indicate that if the JK method is used to analyze SHG experiments in dispersive media the implied high degree of order may be an artifact caused by the inability of the JK method to account properly for the effects that are due to dispersion.

B. Absorption

If the nonlinear material has nonzero absorption for either the fundamental or the SH wave, Eq. (6) will not suffice. In order to introduce the effects of absorption, we write the index of refraction for the nonlinear film as a complex quantity and solve the same boundary-value problem. The effects of absorption have been considered to some extent for electric-field-induced SHG[11] and Maker fringes with wedges[8] and for poled polymer films.[9] By writing the complex index of refraction as $\tilde{n}_m = n_m(1 + i\kappa_m)$, where κ_m is the extinction coefficient of the nonlinear material at the frequency $m\omega$, we arrive at the following expression for the transmitted SH power (neglecting reflections) from an absorbing material:

$$P_{2\omega}^{(\gamma\to p)} = \frac{128\pi^3}{cA}\,\frac{[t_{\mathrm{af}}^{(1\gamma)}]^4[t_{\mathrm{fs}}^{(2p)}]^2[t_{\mathrm{sa}}^{(2p)}]^2}{{n_2}^2{c_2}^2}\,P_\omega^2\left(\frac{2\pi L}{\lambda}\right)^2 {d_{\mathrm{eff}}}^2 \times \exp[-2(\delta_1+\delta_2)]\,\frac{\sin^2\Psi+\sinh^2\chi}{\Psi^2+\chi^2}, \tag{8}$$

where $\chi = \delta_1 - \delta_2 = (2\pi L/\lambda)(n_1\kappa_1/c_1 - n_2\kappa_2/c_2)$. An explanation for the form of δ_i and a complete expression for the SH power including reflections are derived in Appendix B. In general, the transmission factors in Eq. (8) are complex, but for small extinction coefficients they can be considered real.

C. Birefringence

In a uniaxial material the dielectric permittivity is a second-rank tensor and can be represented as

$$\overleftrightarrow{\epsilon}_i = \begin{bmatrix} {n_{\mathrm{io}}}^2 & 0 & 0 \\ 0 & {n_{\mathrm{io}}}^2 & 0 \\ 0 & 0 & {n_{\mathrm{ie}}}^2 \end{bmatrix}, \qquad i = 1, 2, \tag{9}$$

where n_{io} and n_{ie} are the ordinary and the extraordinary indices of refraction at the fundamental ($i = 1$) and the SH ($i = 2$) frequencies, respectively. As detailed in Appendix A, the bound wave[12] for the $p \to p$ case is found to be

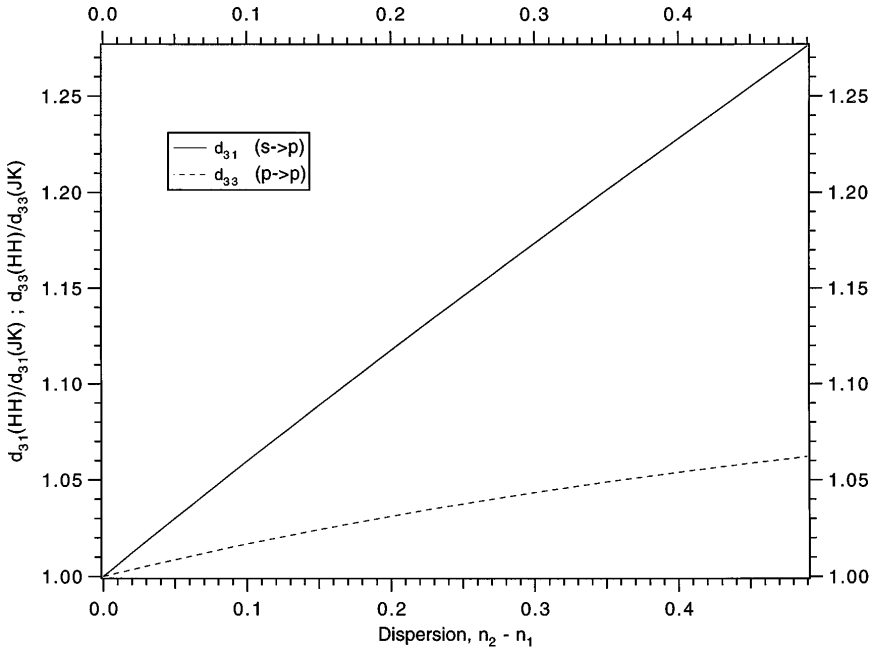

Fig. 3. Ratio of the nonlinear coefficients as obtained by the JK and HH methods.

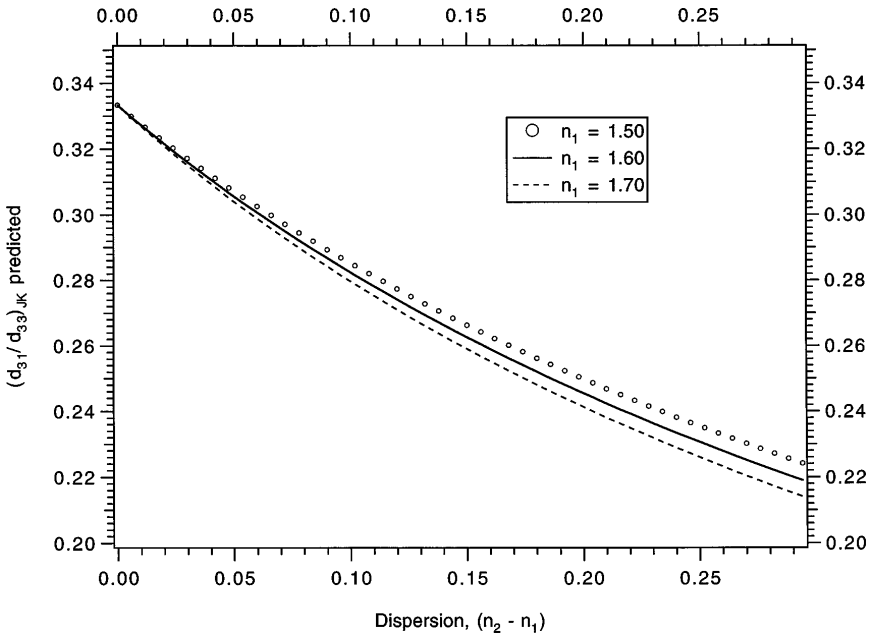

Fig. 4. Effect of dispersion on the ratio d_{31}/d_{33} as calculated with the JK method. $(d_{31}/d_{33})_{\mathrm{HH}}$ is assumed to be 1/3.

$$\mathbf{e}_b = \frac{4\pi {n_2}^2(\theta_1)}{{n_1}^2(\theta_1) - {n_2}^2(\theta_1)} \left[(\vec{\epsilon}_2)^{-1} \cdot \mathbf{P}^{\mathrm{NL}} - \frac{\mathbf{k}_b(\mathbf{k}_b \cdot \mathbf{P}^{\mathrm{NL}})}{\left(\frac{2\omega}{c} n_{2o} n_{2e} \right)^2} \right], \tag{10}$$

where

$$n_i(\theta_i) = \left(\frac{\cos^2 \theta_i}{{n_{\mathrm{io}}}^2} + \frac{\sin^2 \theta_i}{{n_{\mathrm{ie}}}^2} \right)^{-1/2}, \qquad i = 1, 2,$$
$$n_2(\theta_1) = \left(\frac{\cos^2 \theta_1}{{n_{2o}}^2} + \frac{\sin^2 \theta_1}{{n_{2e}}^2} \right)^{-1/2}. \tag{11}$$

A relation for the bound wave similar to Eq. (10) was recently found by Okamoto *et al.*[3,13] To calculate $\mathbf{P}^{\mathrm{NL}}$, and hence d_{eff}, new polarization unit vectors that are functions of the walk-off angle γ (given in Appendix A) must be used. Using these relations, we find that, neglecting reflections, the transmitted SH power from a nonlinear material displaying a uniaxial birefringence is

$$P_{2\omega}^{(\gamma \to p)} = \frac{128\pi^3}{cA} \frac{[t_{\mathrm{af}}^{(1\gamma)}]^4 [t_{\mathrm{fs}}^{(2p)}]^2 [t_{\mathrm{sa}}^{(2p)}]^2}{{n_2}^2(\theta_2) \cos^2 \gamma_2 \cos^2(\theta_2 - \gamma_2)} P_\omega^2 \left(\frac{2\pi L}{\lambda} \right)^2 \times {d_{\mathrm{eff}}}^2 \left[\frac{n_2(\theta_1)}{n_{2o}} \right]^4 \left[\frac{{n_1}^2(\theta_1) - {n_2}^2(\theta_2)}{{n_1}^2(\theta_1) - {n_2}^2(\theta_1)} \right]^2 \frac{\sin^2 \Psi_{\mathrm{bi}}}{{\Psi_{\mathrm{bi}}}^2}, \tag{12}$$

where $\Psi_{\mathrm{bi}} = (2\pi L/\lambda)[n_1(\theta_1)c_1 - n_2(\theta_2)c_2]$ and the Fresnel coefficients for birefringent media are given in Appendix A.

3. RESULTS

We showed above that the JK technique is a good approximation only for the case when $n_1 \approx n_2$. But, as we wish to include any degree of dispersion, when we examine the effects of absorption and birefringence in this section we do so only in terms of the current (HH) theory. We concentrate on those effects from the standpoint of an experimentalist's ability accurately to determine d_{ij} by using the Maker fringe technique. Further, because absorption and birefringence are nearly always present when one is studying organic films and because of the current interest in these materials, we use representative values found in the current literature to illustrate the magnitude of the effects. The theory is not limited to application to these materials, however.

Equation (8) takes the absorption of both the fundamental and the SH waves into effect; however, because most experiments involve doubling from the infrared (where absorption is low) into the visible, we assume no absorption at the fundamental in the following analysis. Although some aspects of absorption in SHG experiments have been considered before, there are two additional features that bear mentioning. The first has to do with the shape of the Maker fringe curve itself for the case of nonzero absorption of the second harmonic. Figure 5 shows the predicted patterns for various levels of absorption of the SH wave for a material with dispersion typical of a side-chain NLO polymer such as Disperse Red 1 methyl methacrylate (DR1-MMA).[14]

The coherence length at a fundamental wavelength of 1064 nm and at normal incidence for the polymer represented in Figs. 5 and 6 is $l_{\mathrm{coh}} = \lambda/4|n_1 - n_2| = 1.24\ \mu$m. This short coherence length gives rise to the Maker fringes seen in the 9-μm-thick film of Fig. 5. However, we see that an absorbance at 2ω of $\alpha_2 = 2\omega n_2 \kappa_2 / c = 0.4/\mu$m causes the fringes to be washed out.

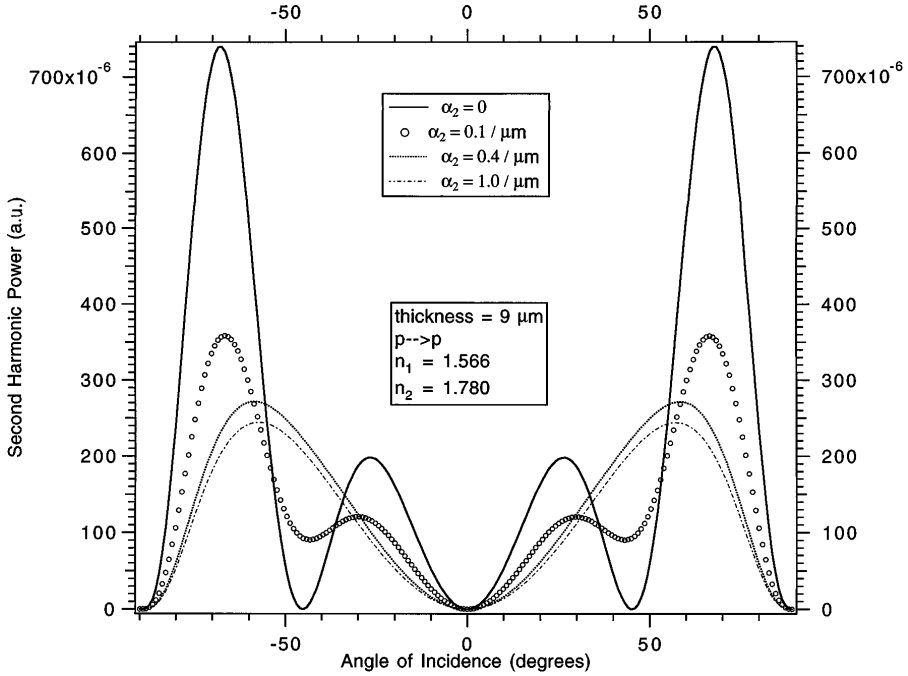

Fig. 5. Maker fringe patterns for a representative absorbing NLO poled polymer.

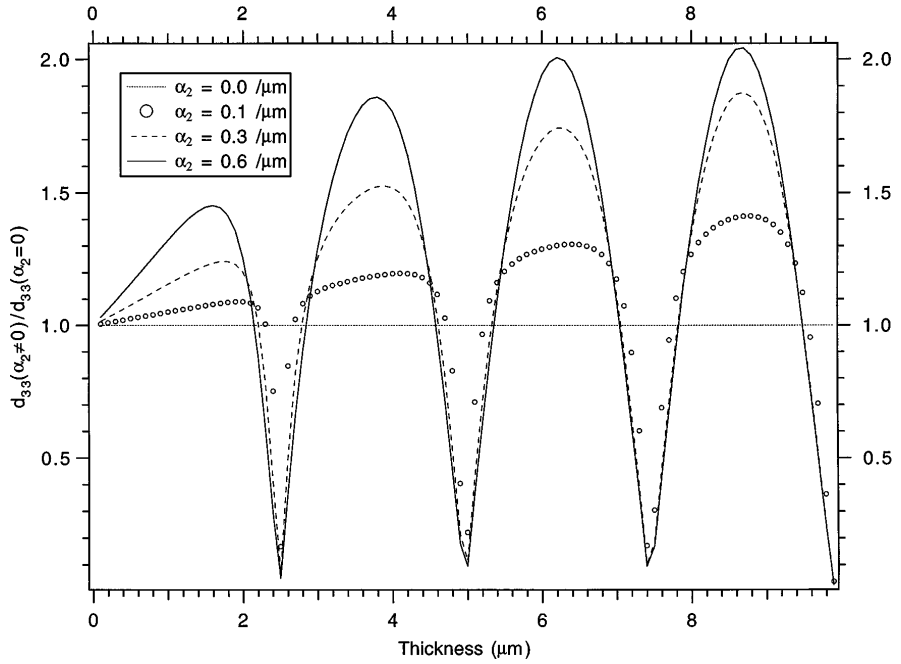

Fig. 6. Effect of absorption on the determination of d_{33} in a NLO polymer. $n_1 = 1.566$, $n_2 = 1.780$, coherence length 1.24 μm.

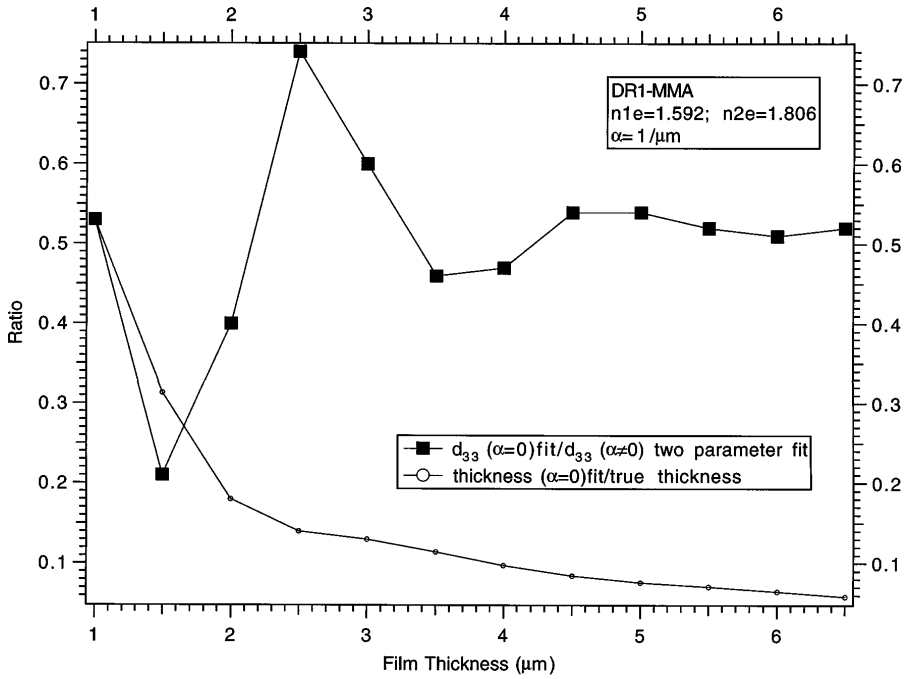

Fig. 7. Ratio of the predicted d_{33} and of the predicted film thickness for the cases of absorption and no absorption. The results are obtained from fits to Eq. (8) (with $\alpha_2 = 0$) for d_{33} and the thickness.

This is due to the dominance of the $\sinh^2 \chi$ term in Eq. (8). No matter what the thickness of the film or its coherence length, a sufficiently high absorbance will completely wash out the fringes and give a curve with one hump, where the shape of the hump is not particularly sensitive to the thickness. This feature of absorbance presents a problem for experimentalists if the thickness and the unit absorbance are not accurately known. The appearance of one hump would normally indicate a film that was of the order of one coherence length thick; hence the resulting fits for d_{ij} would yield erroneous results if the thickness were not accurately known from other means.

The second feature of interest concerning the effects of absorption on Maker fringe experiments is shown in Fig. 6. In this figure we compare the predicted values of d_{33} obtained with and without consideration for the effects of absorption. In addition to the expected general trend of underestimation of d_{33} we see that, for any level of absorption, a dramatic overestimation is possible if the material thickness is near an even multiple of the

coherence length. These results are found by comparison of the SH intensities of the two cases at an angle of incidence of 50°.

This plot emphasizes the need to perform the full angular scan and fit the results to the theory. By considering data generated by Eq. (8) with $\alpha_2 = 1/\mu$m, we have calculated the difference in the predicted values of the film thickness and d_{33} for the two cases. Besides the fact that the fitted parameters calculated by neglecting absorption are very inaccurate, Fig. 7 shows that in order to fit the data one must adjust the fitted thickness to successively smaller values, while the fitted d_{33} settles on a value of ~50% of the true value for all film thicknesses >4 μm for the chosen polymer parameters. As a result, one can see that, if absorption is not taken into account, the fitted d_{33} is independent of thickness after the thickness increases above a certain amount.

We start our discussion on the effect of birefringence by examining the Maker fringe plot for each case for X-cut quartz. Figure 8 shows only a slight difference between the two cases. Calculation of d_{11} and the crystal thickness for each case yields a difference of 2% and 2 μm, respectively, for a 1000-μm-thick crystal. The close agreement between the isotropic and birefringent treat-

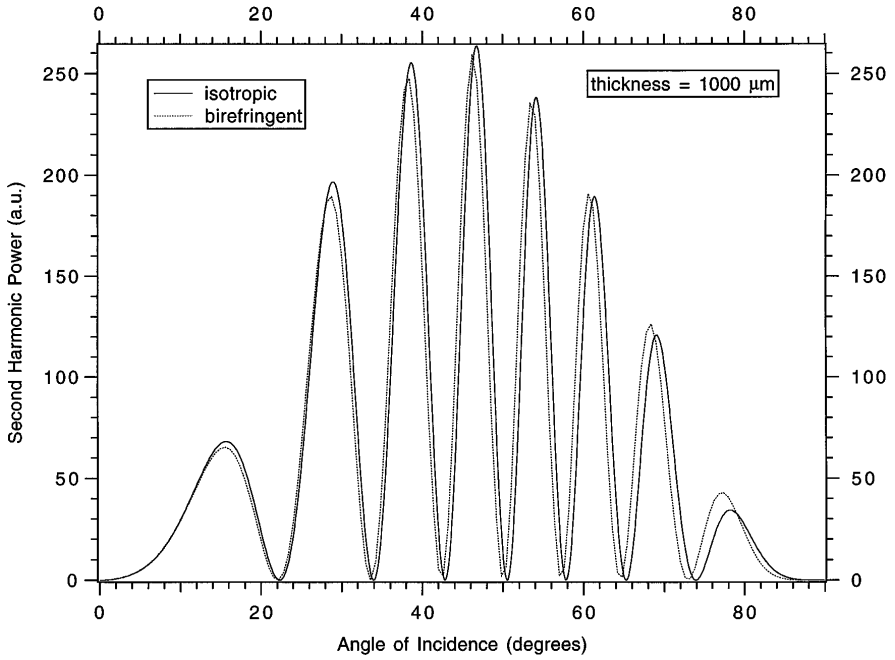

Fig. 8. Maker fringe plots for 1000-μm-thick X-cut quartz.

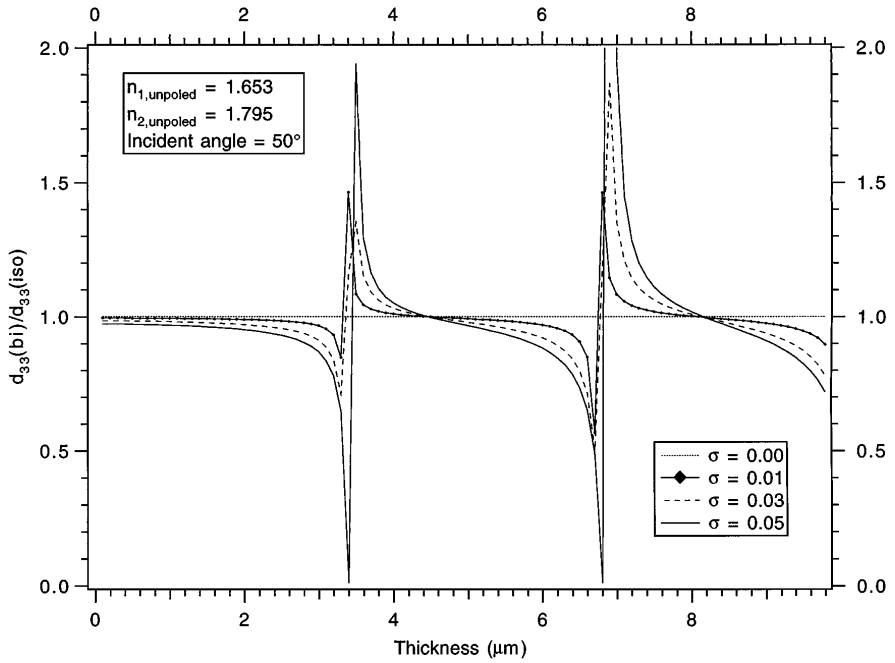

Fig. 9. Effect of birefringence on the calculation of d_{33} in a poled polymer. Extraordinary indices were used for the isotropic case.

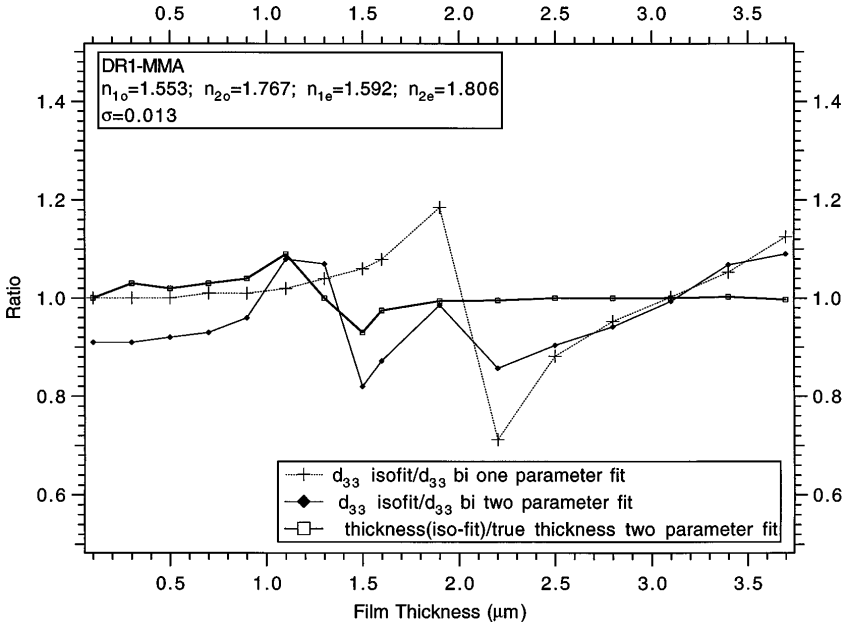

Fig. 10. Ratio of the predicted d_{33} and film thickness for the isotropic and the birefringent cases. The results are obtained from fits to Eq. (12) for d_{33} (crosses) and d_{33} and the thickness (filled diamonds and open boxes).

ments is due to the small birefringence of quartz. Quartz has a birefringence ($\Delta n_i \equiv n_{ie} - n_{io} = 3\sigma_i$) of 0.0088 and 0.0091 at 1.064 and 0.532 μm, respectively.

The standard definition of birefringence, Δn, can be related to the poling-induced birefringence in polymers, σ_i, through the following relations:

$$n_{io} = n_{iu} - \sigma_i\,,$$
$$n_{ie} = n_{iu} + 2\sigma_i\,, \tag{13}$$

where $i = 1, 2$ and n_{iu} is the unpoled index at the frequency $i\omega$. Equations (13) are generally valid for amorphous poled polymers. Recent data for poling-induced birefringence in a polymer (bisphenol-A 4–amino-4′-nitrotolane, $\sigma_i = 0.020 \rightarrow 0.025$) are given by Jungbauer *et al.*[15] In Fig. 9 we have calculated the ratio of d_{33} (birefringent)/d_{33} (isotropic) as a function of film thickness and degree of birefringence for an incident angle of 50°.

The use of the ordinary indices gives qualitative results similar to those in Fig. 9, but the magnitude of the error is worse than the result from use of the extraordinary indices for a $p \rightarrow p$ experiment. Figure 9 also shows us that experiments that attempt to determine d_{33} while making comparisons at only a single angle and ignoring birefringence are subject to very large errors that depend on the thickness of the film, regardless of the degree of birefringence. We have also calculated d_{33} from isotropic fits of complete angular test data generated with the full birefringent theory. Figure 10 shows these results as a function of film thickness when the index data ($\sigma = 0.013$) for a typical DR1-MMA side chain are used.[14] We are making two different comparisons in this plot. First we assume that the thickness is accurately known and let d_{33} vary alone. This results in fairly significant differences from the true values of d_{33}. Next we allow the film thickness to vary also. The ratio of the fitted thickness to the true thickness is seen to be quite close to 1 for all thicknesses greater than approximately two coherence lengths. In this range the fitted value of d_{33} is closer to the true value than for the first case when the thickness was fixed, but it is still appreciably different. For thicknesses less than two coherence lengths there is a wide deviation from the true values for both the thickness and d_{33}. The use of the full birefringent theory is clearly called for if accurate determination of d_{ij} is sought.

4. CONCLUSIONS

In this paper we have presented new expressions for analyzing data from Maker fringe SHG experiments. These expressions include the effects of reflections of the SH wave in the nonlinear material and are valid for any angle of incidence or degree of dispersion. We have shown that neglecting the reflections after solving for the SH power is preferred to doing so in the boundary conditions when setting up the problem, because the results are more generally applicable to systems with dispersion. Furthermore, we show that the use of the JK theory rather than the HH theory can result in an underestimation of the ratio d_{31}/d_{33} in experiments in which dispersion is a factor.

We have also included the effects of absorption of the fundamental and SH waves by the nonlinear media. When dealing with an absorbing material, the best advice for experimentalists is to perform the experiment far from the resonances of the nonlinear material. However, this is not always possible, and for such a case our results show that an accurate determination of the thickness and absorption coefficient is required if one is to get meaningful results.

We have also presented, for the first time to our knowledge, an accurate extension of the Maker fringe technique to birefringent materials. By applying that theory to representative materials studied today, we have shown that large discrepancies in the prediction of d_{ij} can result if birefringence is neglected. There does not appear to be

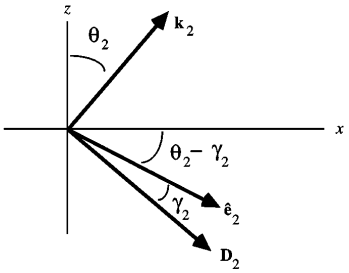

Fig. 11. Definition of the walk-off angle γ in a birefringent medium.

any reason to ignore the effects of birefringence, given the simple nature and form of the theory that handles it.

The remaining task necessary for a complete theory for use in analyzing Maker fringe experiments is to include the combined effects of absorption and birefringence.

APPENDIX A: BIREFRINGENCE

Here we derive the expression for the SH power generated in a birefringent nonlinear film. We assume no depletion of the fundamental. Maxwell's equations require that the SH field $\mathbf{E}_2$ satisfy

$$\nabla\times\nabla\times\mathbf{E}_2-\left(\frac{2\omega}{c}\right)^2\vec{\epsilon}_2\cdot\mathbf{E}_2=\left(\frac{2\omega}{c}\right)^2 4\pi\mathbf{P}^{\mathrm{NL}}\exp(2i\mathbf{k}_1\cdot\mathbf{r}), \tag{A1}$$

where use is made of the electric displacement vector $\mathbf{D}_2=\vec{\epsilon}_2\cdot\mathbf{E}_2+4\pi\mathbf{P}^{\mathrm{NL}}\exp(2i\mathbf{k}_1\cdot\mathbf{r})$, $\vec{\epsilon}$ is the permittivity tensor given in Eq. (9), and $\mathbf{P}^{\mathrm{NL}}$ is given in Eqs. (5). In the linear media (air, substrate), $\mathbf{P}^{\mathrm{NL}}$ is zero and Eq. (A1) is homogeneous.

In the nonlinear film (Region II of Fig. 1), the propagation vectors that appear in Eqs. (3) for the $p\rightarrow p$ case take the forms

$$\mathbf{k}_m=\frac{m\omega n_m(\theta_m)}{c}(s_m,\,0,\,c_m),\qquad m=1,\,2,$$

$$\mathbf{k}_2^r=\frac{2\omega n_2(\theta_2)}{c}(s_2,\,0,\,-c_2), \tag{A2}$$

with the angle-dependent refractive indices $n_m(\theta_m)$ given in Eqs. (11). Although $\mathbf{D}_2$ is still perpendicular to $\mathbf{k}_2$, the electric field deviates from the perpendicular by the walk-off angle[16] γ, as shown in Fig. 11.

The unit vectors that describe the **E**-field polarization are then given by

$$\hat{\mathbf{e}}_m=[\cos(\theta_m-\gamma_m),\,0,\,-\sin(\theta_m-\gamma_m)],\qquad m=1,2$$

$$\hat{\mathbf{e}}_2^r=[-\cos(\theta_2-\gamma_2),\,0,\,-\sin(\theta_2-\gamma_2)]. \tag{A3}$$

Using $\mathbf{D}=\vec{\epsilon}\cdot\mathbf{E}$ and $\mathbf{D}=[n(\theta)/c]^2\hat{\mathbf{k}}\times(\mathbf{E}\times\hat{\mathbf{k}})$ for the linear electric displacement field, we can derive the following useful relations:

$$\cos(\theta_m-\gamma_m)=\left[\frac{n_m(\theta_m)}{n_{\mathrm{mo}}}\right]^2\cos\gamma_m\cos\theta_m,$$

$$\sin(\theta_m-\gamma_m)=\left[\frac{n_m(\theta_m)}{n_{\mathrm{me}}}\right]^2\cos\gamma_m\sin\theta_m, \tag{A4}$$

$$\tan\gamma_m=\frac{1}{2}n_m(\theta_m)^2\sin 2\theta_m\left(\frac{1}{n_{\mathrm{mo}}{}^2}-\frac{1}{n_{\mathrm{me}}{}^2}\right). \tag{A5}$$

Furthermore, because $\hat{\mathbf{e}}_m\cdot\hat{\mathbf{e}}_m=1$, we have

$$\cos\gamma_m=\frac{n_{\mathrm{mo}}n_{\mathrm{me}}}{n_m(\theta_m)[n_{\mathrm{mo}}{}^2+n_{\mathrm{me}}{}^2-n_m(\theta_m)^2]^{1/2}}. \tag{A6}$$

The angles θ_m in the birefringent film are obtained by use of Eq. (11) in conjunction with Snell's law, $n_m(\theta_m)\sin\theta_m=\sin\theta$, to get

$$\sin\theta_m=\frac{n_{\mathrm{me}}\sin\theta}{[(n_{\mathrm{mo}}n_{\mathrm{me}})^2+(n_{\mathrm{me}}{}^2-n_{\mathrm{mo}}{}^2)\sin^2\theta]^{1/2}}. \tag{A7}$$

For the $s\rightarrow p$ case the fundamental beam is s polarized, so that $\gamma_1=0$ and

$$\mathbf{k}_1=(\omega/c)n_{1o}(s_1,\,0,\,c_1),$$

$$\hat{\mathbf{e}}_1=(0,\,1,\,0),$$

$$\sin\theta_1=\sin\theta/n_{1o}, \tag{A8}$$

while Eqs. (A2)–(A8) remain valid for the SH wave ($m=2$).

The bound wave, $\mathbf{E}_{2b}$, is a particular solution to the inhomogeneous equation (A1) in the nonlinear material.[17] Inserting $\mathbf{E}_{2b}=\mathbf{e}_b\exp(i\mathbf{k}_b\cdot\mathbf{r})$, with $\mathbf{k}_b=2\mathbf{k}_1$, into Eq. (A1) gives the following equations for the bound wave amplitude $\mathbf{e}_b$:

$$[-n_1{}^2(\theta_1)c_1{}^2+n_{2o}{}^2]e_{bx}+n_1{}^2(\theta_1)s_1c_1e_{bz}=-4\pi P_x^{\mathrm{NL}},$$

$$n_1{}^2(\theta_1)c_1s_1e_{bx}+[-n_1{}^2(\theta_1)s_1{}^2+n_{2e}{}^2]e_{bx}=-4\pi P_z^{\mathrm{NL}}. \tag{A9}$$

On solving for e_{bx} and e_{bz}, one can conveniently write the solution as in Eq. (10).

The total fields in each of the three regions are as given in Eqs. (2)–(4), with the exception of $\mathbf{H}_2$ in Eq. (3), which for birefringence is given by

$$\mathbf{H}_2=\mathbf{h}_b\exp(i2\mathbf{k}_1\cdot\mathbf{r})+n_2(\theta_2)\cos\gamma_2[A\hat{\mathbf{e}}_{2s}\exp(i\mathbf{k}_2\cdot\mathbf{r})+B\hat{\mathbf{e}}_{2s}^r\exp(i\mathbf{k}_{2r}\cdot\mathbf{r})], \tag{A10}$$

where $\mathbf{h}_b=n_1(\theta_1)\mathbf{k}_1\times\mathbf{e}_b$ and the bound wave $\mathbf{e}_b$ is given in Eq. (10). The boundary conditions at the I–II interface ($z=-L/2$) requiring the continuity of E_{2x} and H_{2y} result in the equations

$$-\cos(\theta)R=e_{bx}\exp(-i\phi_1)+\cos(\theta_2-\gamma_2)\times[A\exp(-i\phi_2)-B\exp(i\phi_2)], \tag{A11}$$

$$R=h_{by}\exp(-i\phi_1)+n_2(\theta_2)\cos\gamma_2\times[A\exp(-i\phi_2)+B\exp(i\phi_2)], \tag{A12}$$

respectively. Continuity of these field components at the II–III interface ($z=L/2$) yields

$$c_{2s}T=e_{bx}\exp(i\phi_1)+\cos(\theta_2-\gamma_2)\times[A\exp(i\phi_2)-B\exp(-i\phi_2)], \tag{A13}$$

$$n_{2s}T=h_{by}\exp(i\phi_1)+n_2(\theta_2)\cos\gamma_2\times[A\exp(i\phi_2)+B\exp(-i\phi_2)], \tag{A14}$$

where $\phi_1=k_1c_1L$ and $\phi_2=k_2c_2L/2$. Note that, in the JK approach, $B=0$ in Eqs. (A11)–(A14). Solving

Eqs. (A11)–(A14) for A and B and inserting the results into the equation for T, obtained by multiplying Eq. (A13) by n_{2s} and Eq. (A14) by c_{2s} and adding, we obtain the transmitted field

$$T = (1/\Delta)[-u_a^+ v^+ \exp(\phi_1 - 2\phi_2) + u_a^- v^- \exp(\phi_1 + 2\phi_2) + 2n_2(\theta_2)\cos\gamma_2 \cos(\theta_2 - \gamma_2)(h_{by}\cos\theta + e_{bx}) \times \exp(-i\phi_1)], \tag{A15}$$

where

$$\Delta = -u_a^+ u_s^+ \exp(-2i\phi_2) + u_a^- u_s^- \exp(2i\phi_2), \tag{A16}$$

$$u_a^\pm = \cos(\theta_2 - \gamma_2) \pm n_2(\theta_2)\cos\gamma_2 \cos\theta,$$
$$u_s^\pm = n_{2s}\cos(\theta_2 - \gamma_2) \pm n_2(\theta_2)c_{2s}\cos\gamma_2,$$
$$v^\pm = h_{by}\cos(\theta_2 - \gamma_2) \pm n_2(\theta_2)e_{bx}\cos\gamma_2. \tag{A17}$$

When the identities

$$\exp i(\phi_1 \pm 2\phi_2) = 2i\sin(\phi_1 \pm \phi_2)\exp(\pm i\phi_2) + \exp(-i\phi_1) \tag{A18}$$

are used in Eq. (A15), the terms proportional to $\exp(-i\phi_1)$ cancel out (unlike when JK-type boundary conditions are used). Furthermore, from Eqs. (9) and (A12) we find that

$$v^\pm = \frac{4\pi n_2(\theta_1)^2}{n_1(\theta_1)^2 - n_2(\theta_1)^2} \frac{[n_1(\theta_1)c_1 \pm n_2(\theta_2)c_2]}{{n_{2o}}^2} \begin{Bmatrix} \hat{\mathbf{e}}_2 \cdot \mathbf{P}^{\mathrm{NL}} \\ \hat{\mathbf{e}}_2^r \cdot \mathbf{P}^{\mathrm{NL}} \end{Bmatrix}, \tag{A19}$$

after considerable simplification requiring Eqs. (11), (A3), and (A4). Thus, use of Eqs. (A18) and (A19) in Eq. (A15) gives

$$T = -\frac{8\pi i}{\Delta}\left[\frac{n_2(\theta_1)}{n_{2o}}\right]^2 \frac{1}{n_1(\theta_1)^2 - n_2(\theta_2)^2} \times \{u_a^+[n_1(\theta_1)c_1 + n_2(\theta_2)c_2]\hat{\mathbf{e}}_2 \cdot \mathbf{P}^{\mathrm{NL}} \sin(\phi_1 - \phi_2) \times \exp(-i\phi_2) + u_a^-[n_1(\theta_1)c_1 - n_2(\theta_2)c_2]\hat{\mathbf{e}}_2^r \cdot \mathbf{P}^{\mathrm{NL}} \times \sin(\phi_1 + \phi_2)\exp(i\phi_2)\}. \tag{A20}$$

The p-polarized reflection coefficients at the air–film and film–substrate interfaces for the SH wave are

$$r_{\mathrm{af}}^{(2p)} = -u_a^-/u_a^+, \qquad r_{\mathrm{fs}}^{(2p)} = u_s^-/u_s^+, \tag{A21}$$

whereas the transmission coefficient for the SH wave at the film–substrate interface is

$$t_{\mathrm{fs}}^{(2p)} = \frac{2n_2(\theta_2)\cos\gamma_2\cos(\theta_2 - \gamma_2)}{u_s^+}. \tag{A22}$$

Then the use of Eqs. (A21), (A22), and (A16) in Eq. (A20), together with

$$n_1(\theta_1)^2 - n_2(\theta_2)^2 = [n_1(\theta_1)c_1 + n_2(\theta_2)c_2] \times [n_1(\theta_1)c_1 - n_2(\theta_2)c_2], \tag{A23}$$

which holds because of Snell's law, gives

$$T = \frac{4\pi i t_{\mathrm{fs}}^{(2p)}}{n_2(\theta_2)\cos\gamma_2\cos(\theta_2 - \gamma_2)}\left(\frac{2\pi L}{\lambda}\right)\left[\frac{n_2(\theta_1)}{n_{2o}}\right]^2\left[\frac{n_1(\theta_1)^2 - n_2(\theta_2)^2}{n_1(\theta_1)^2 - n_2(\theta_1)^2}\right] \times \frac{\left[\hat{\mathbf{e}}_2 \cdot \mathbf{P}^{\mathrm{NL}} \frac{\sin\Psi_{\mathrm{bi}}}{\Psi_{\mathrm{bi}}} \exp(-i\phi_2) - r_{\mathrm{af}}^{(2p)}\hat{\mathbf{e}}_2^r \cdot \mathbf{P}^{\mathrm{NL}} \frac{\sin\Phi_{\mathrm{bi}}}{\Phi_{\mathrm{bi}}} \exp(i\phi_2)\right]}{[\exp(-2i\phi_2) + r_{\mathrm{af}}^{(2p)} r_{\mathrm{fs}}^{(2p)} \exp(2i\phi_2)]}, \tag{A24}$$

where

$$\Psi_{\mathrm{bi}} = \phi_1 - \phi_2 = \frac{2\pi L}{\lambda}[n_1(\theta_1)c_1 - n_2(\theta_2)c_2],$$
$$\Phi_{\mathrm{bi}} = \phi_1 + \phi_2 = \frac{2\pi L}{\lambda}[n_1(\theta_1)c_1 + n_2(\theta_2)c_2]. \tag{A25}$$

The components of $\mathbf{P}^{\mathrm{NL}}$ along the SH $\mathbf{E}$ fields are given by

$$\hat{\mathbf{e}}_2 \cdot \mathbf{P}^{\mathrm{NL}} = -\frac{8\pi}{c} d_{\mathrm{eff}} I_1 [t_{\mathrm{af}}^{(1\gamma)}]^2,$$
$$\hat{\mathbf{e}}_2^r \cdot \mathbf{P}^{\mathrm{NL}} = -\frac{8\pi}{c} d_{\mathrm{eff}}^r I_1 [t_{\mathrm{af}}^{(1\gamma)}]^2, \tag{A26}$$

where I_1 is the intensity of the incident fundamental wave, $t_{\mathrm{af}}^{(1\gamma)}$ is the transmission coefficient for the fundamental at the air–film interface,

$$t_{\mathrm{af}}^{(1\gamma)} = \begin{cases} \dfrac{2\cos\theta}{\cos(\theta_1 - \gamma_1) + n_1(\theta_1)\cos\gamma_1\cos\theta}, & \gamma = p \\ \dfrac{2\cos\theta}{\cos\theta_1 + n_{1o}\cos\theta}, & \gamma = s \end{cases}, \tag{A27}$$

and the effective d coefficients for $C_{\infty v}$ space symmetry are

$$d_{\mathrm{eff}} = -\hat{\mathbf{e}}_2 \cdot \vec{\mathbf{d}} : \hat{\mathbf{e}}_1\hat{\mathbf{e}}_1 = \begin{cases} d_{14}\cos(\theta_2 - \gamma_2)\sin 2(\theta_1 - \gamma_1) + \sin(\theta_2 - \gamma_2)[d_{31}\cos^2(\theta_1 - \gamma_1) + d_{33}\sin^2(\theta_1 - \gamma_1)] & p \to p, \\ d_{31}\sin(\theta_2 - \gamma_2), & s \to p \end{cases}$$
$$d_{\mathrm{eff}}^r = -\hat{\mathbf{e}}_2^r \cdot \vec{\mathbf{d}} : \hat{\mathbf{e}}_1\hat{\mathbf{e}}_1 = \begin{cases} -d_{15}\cos(\theta_2 - \gamma_2)\sin 2(\theta_1 - \gamma_1) + \sin(\theta_2 - \gamma_2)[d_{31}\cos^2(\theta_1 - \gamma_1) + d_{33}\sin^2(\theta_1 - \gamma_1)], & p \to p \\ d_{31}\sin(\theta_2 - \gamma_2), & s \to p \end{cases}. \tag{A28}$$

The SH power transmitted through the substrate into air is then given by $c/8\pi[t_{\mathrm{sa}}^{(2p)}]^2|T|^2A$, where A is the cross-sectional area of the fundamental beam, and the transmission coefficient for the p-polarized SH wave from the substrate into air is

$$t_{\mathrm{sa}}^{(2p)} = \frac{2n_{2s}c_{2s}}{n_{2s}\cos\theta + c_{2s}}. \tag{A29}$$

Thus we get

$$P_{2\omega}^{\gamma\to p} = \frac{128\pi^3}{cA}\frac{[t_{\rm sa}^{(2p)}]^2[t_{\rm fs}^{(2p)}]^2[t_{\rm af}^{(1\gamma)}]^4P_\omega^2}{n_2(\theta_2)^2\cos^2\gamma_2\cos^2(\theta_2-\gamma_2)}\left(\frac{2\pi L}{\lambda}\right)^2\left[\frac{n_2(\theta_1)}{n_{2o}}\right]^4\left[\frac{n_1(\theta_1)^2-n_2(\theta_2)^2}{n_1(\theta_1)^2-n_2(\theta_1)^2}\right]^2$$
$$\times {d_{\rm eff}}^2\frac{\left\{\frac{\sin^2\Psi_{\rm bi}}{\Psi_{\rm bi}^2}+[r_{\rm af}^{(2p)}]^2R^2\frac{\sin^2\Phi_{\rm bi}}{\Phi_{\rm bi}^2}-2r_{\rm af}^{(2p)}R\frac{\sin\Psi_{\rm bi}}{\Psi_{\rm bi}}\frac{\sin\Phi_{\rm bi}}{\Phi_{\rm bi}}\cos 2\phi_2\right\}}{\{1+[r_{\rm af}^{(2p)}r_{\rm fs}^{(2p)}]^2+2r_{\rm af}^{(2p)}r_{\rm fs}^{(2p)}\cos 4\phi_2\}}, \quad \text{(A30)}$$

where R is the ratio ${d_{\rm eff}}^r/d_{\rm eff}$. For the case of $s\to p$ generation, the bound waves $\mathbf{e}_b$ and $\mathbf{h}_b$ are given by Eqs. (10) and (A10) with the substitution $n_1(\theta_1)\to n_{1o}$. This substitution in Eq. (A30) gives the corresponding SH power. We obtain the isotropic result, Eq. (6), from Eq. (A30) by letting $n_{1e}=n_{1o}\to n_1$ and $n_{2e}=n_{2o}\to n_2$.

APPENDIX B. ABSORPTION

For an isotropic, absorbing nonlinear material, the fields in the three regions are given by Eqs. (2)–(5) but with complex refractive indices[18] $\tilde n_m = n_m(1+i\kappa_m)$. Snell's law for a transparent medium (n) to an absorbing medium ($\tilde n$), $\tilde n\sin\tilde\theta = n\sin\theta$, then implies complex angles of refraction, $\tilde\theta=\theta_r+i\theta_i$. We can separate Snell's law into real and imaginary parts in order to solve for θ_r and θ_i. We obtain

$$\tanh\theta_i = -\kappa\tan\theta_r, \quad \text{(B1)}$$
$$\cos^2\theta_r = \frac{(\cos^2\theta_R+\kappa^2)+[(\cos^2\theta_R-\kappa^2)^2+4\kappa^2]^{1/2}}{2(1+\kappa^2)}, \quad \text{(B2)}$$

where θ_R is the angle of refraction in the limit $\kappa\to 0$, viz., $\sin\theta_R = n\sin\theta/n_m$. We also need the product $\tilde n\cos\tilde\theta$. Expansion of this product into real and imaginary parts and subsequent use of Eq. (B1) gives

$$\tilde n\cos\tilde\theta = \frac{n\cos\theta_r}{\cosh\theta_i}+i\frac{n\kappa}{\cos\theta_r}\cosh\theta_i. \quad \text{(B3)}$$

For small κ, θ_r is only slightly larger than θ_R. For example, for $n=1.6$, $\kappa=0.06$, and at a large incident angle of 80° we calculate $\theta_R=\sin^{-1}(\sin 80/1.6)=38.0°$, $\theta_r=38.2°$ [from Eq. (B2)], and $\cosh\theta_i=1.001$ [from Eq. (B2)]. Then, as $\cosh\theta_i\approx 1$ and $\theta_r\approx\theta_R$, Eq. (B3) can be written as

$$\tilde n\cos\tilde\theta \approx n\cos\theta_R + in\kappa/\cos\theta_R. \quad \text{(B4)}$$

We shall subsequently use this approximation in terms involving phase and assume real angles in transmission and reflection coefficients. Applying the same boundary conditions as in Appendix A, we obtain

$$T = \frac{4\pi i t_{\rm fs}^{(2p)}}{n_2c_2}\left(\frac{2\pi L}{\lambda}\right)\frac{\left[\hat{\mathbf{e}}_2\cdot\mathbf{P}^{\rm NL}\frac{\sin\tilde\Psi}{\tilde\Psi}\exp(-i\tilde\phi_2)-r_{\rm af}^{(2p)}\hat{\mathbf{e}}_2^r\cdot\mathbf{P}^{\rm NL}\frac{\sin\tilde\Phi}{\tilde\Phi}\exp(i\tilde\phi_2)\right]}{[\exp(-2i\tilde\phi_2)+r_{\rm af}^{(2p)}r_{\rm fs}^{(2p)}\exp(2i\tilde\phi_2)]}, \quad \text{(B5)}$$

where, with the aid of Eq. (B4),

$$\tilde\phi_m = \frac{2\pi L}{\lambda}\tilde n_m\tilde c_m = \phi_m+i\delta_m, \qquad \delta_m = \frac{2\pi L}{\lambda}\frac{n_m\kappa_m}{c_m}, \quad \text{(B6)}$$

$$\tilde\Psi = \tilde\phi_1-\tilde\phi_2 = \Psi+i\chi, \qquad \chi = \frac{2\pi L}{\lambda}\left(\frac{n_1\kappa_1}{c_1}-\frac{n_2\kappa_2}{c_2}\right), \quad \text{(B7)}$$

$$\tilde\Phi = \tilde\phi_1+\tilde\phi_2 = \Phi+i\Gamma, \qquad \Gamma = \frac{2\pi L}{\lambda}\left(\frac{n_1\kappa_1}{c_1}+\frac{n_2\kappa_2}{c_2}\right), \quad \text{(B8)}$$

and the transmission and reflection coefficients are

$$t_{\rm fs}^{(2p)} = \frac{2n_2c_2}{n_{2s}c_2+n_2c_{2s}},$$
$$r_{\rm af}^{(2p)} = \frac{n_2\cos\theta-c_2}{n_2\cos\theta+c_2},$$
$$r_{\rm fs}^{(2p)} = \frac{n_{2s}c_2-n_2c_{2s}}{n_{2s}c_2+n_2c_{2s}}. \quad \text{(B9)}$$

For the case of absorption, $\mathbf{e}_b$ in Eqs. (3) is the value of the bound wave amplitude at the middle of the film. Consequently, $\mathbf{P}^{\rm NL}$ in Eqs. (5) depends on the fundamental wave amplitude at the center of the film, viz.,

$$\mathbf{P}^{\rm NL} = |E_1|^2\vec{\mathbf{d}}:[\hat{\mathbf{e}}_1\exp(-\delta_1/2)][\hat{\mathbf{e}}_1\exp(-\delta_1/2)], \quad \text{(B10)}$$

where E_1 is the magnitude of the fundamental wave in air. Using Eq. (B10) in $P_{2\omega}=(c/8\pi)[t_{\rm sa}^{(2p)}]^2|T|^2A$, with T given by Eq. (B5), we obtain

$$P_{2\omega}^{(\gamma\to p)} = \frac{128\pi^3}{cA}\frac{[t_{\rm sa}^{(2p)}]^2[t_{\rm fs}^{(2p)}]^2[t_{\rm af}^{(1\gamma)}]^4P_\omega^2}{{n_2}^2{c_2}^2}\left(\frac{2\pi L}{\lambda}\right)^2{d_{\rm eff}}^2\exp[-2(\delta_1+\delta_2)]$$
$$\times\frac{\left\{|\sin\tilde\Psi/\tilde\Psi|^2+[r_{\rm af}^{(2p)}]^2R^2\exp(-4\delta_2)|\sin\tilde\Phi/\tilde\Phi|^2-2r_{\rm af}^{(2p)}R\exp(-2\delta_2)|\sin\tilde\Psi/\tilde\Psi||\sin\tilde\Phi/\tilde\Phi|\cos(2\phi_2-\theta_x+\theta_y)\right\}}{\{1+[r_{\rm af}^{(2p)}r_{\rm fs}^{(2p)}]^2\exp(-8\delta_2)+2r_{\rm af}^{(2p)}r_{\rm fs}^{(2p)}\cos 4\phi_2\exp(-4\delta_2)\}}, \quad \text{(B11)}$$

where

$$|\sin\tilde\Psi/\tilde\Psi|^2 = (\sin^2\Psi+\sinh^2\chi)/(\Psi^2+\chi^2),$$
$$|\sin\tilde\Phi/\tilde\Phi|^2 = (\sin^2\Phi+\sinh^2\Gamma)/(\Phi^2+\Gamma^2),$$
$$\tan\theta_x = \frac{\Psi\tanh\chi-\chi\tan\Psi}{\Psi\tan\Psi+\chi\tanh\chi},$$
$$\tan\theta_y = \frac{\Phi\tanh\Gamma-\Gamma\tan\Phi}{\Phi\tan\Phi+\Gamma\tanh\Gamma}, \quad \text{(B12)}$$

and $R = d^r_{\text{eff}}/d_{\text{eff}}$ with d_{eff} and d^r_{eff} given as in Eq. (A28) but with $\gamma_1 = \gamma_2 = 0$.

ACKNOWLEDGMENTS

W. N. Herman gratefully acknowledges the support of the U.S. Office of Naval Research. L. M. Hayden thanks the U.S. Naval Academy for partial support for this work.

Note added in proof: We do not include the effects of multiple reflections of the fundamental here, although Neher *et al.*[19] has included them for the case of third-harmonic generation. They found that, for the case in which the nonlinear film is on the side of the substrate facing the incident beam (as in this paper), the effect of neglecting the multiple reflections of the fundamental is small.

REFERENCES AND NOTES

1. P. D. Maker, R. W. Terhune, M. Nisenhoff, and C. M. Savage, Phys. Rev. Lett. **8,** 21 (1962).
2. J. Jerphagnon and S. K. Kurtz, "Maker fringes: a detailed comparison of theory and experiment for isotropic and uniaxial crystals," J. Appl. Phys. **41,** 1667 (1970).
3. N. Okamoto, Y. Hirano, and O. Sugihara, "Precise estimation of nonlinear-optical coefficients for anisotropic nonlinear films with $C_{\infty v}$ symmetry," J. Opt. Soc. Am. B **9,** 2083 (1992).
4. M. Eich, B. Reck, D. Y. Yoon, C. G. Willson, and G. C. Bjorklund, "Novel second-order nonlinear optical polymers via chemical cross-linking-induced vitrification under electric field," J. Appl. Phys. **66,** 3241 (1989).
5. C. H. Wang and H. W. Guan, "Second harmonic generation and optical anisotropy of a spin cast polymer film," J. Polym. Sci. Part B **31,** 1983 (1993).
6. M. G. Kuzyk, K. D. Singer, H. E. Zahn, and L. A. King, "Second-order nonlinear-optical tensor properties of poled films under stress," J. Opt. Soc. Am. B **6,** 742 (1989).
7. N. Bloembergen and P. S. Pershan, "Light waves at the boundary of nonlinear media," Phys. Rev. **128,** 606 (1962).
8. D. Chemla and P. Kupecek, "Analyse des expériences de génération de second harmonique," Rev. Phys. Appl. **6,** 31 (1971).
9. L. M. Hayden, G. F. Sauter, F. R. Ore, P. L. Pasillas, J. M. Hoover, G. A. Lindsay, and R. A. Henry, "Second-order nonlinear optical measurements in guest-host and side-chain polymers," J. Appl. Phys. **68,** 456 (1990).
10. D. J. Williams, "Nonlinear optical properties of guest-host polymer structures," in *Nonlinear Optical Properties of Organic Molecules and Crystals*, D. S. Chemla and J. Zyss, eds. (Academic, Orlando, Fla., 1987), p. 405.
11. J. L. Oudar, "Optical nonlinearities of conjugated molecules. Stilbene derivatives and highly polar aromatic compounds," J. Chem. Phys. **67,** 446 (1977).
12. The anisotropic bound wave is also discussed in Ref. 8.
13. In Ref. 3 Eq. (18) must be corrected so that the denominator divides only the second term in the numerator.
14. A. Nahata, J. Shan, J. T. Yardley, and C. Wu, "Electro-optic determination of the nonlinear-optical properties of a covalently functionalized Disperse Red 1 copolymer," J. Opt. Soc. Am. B **10,** 1553 (1993). [The same material with a different dye content, Poly(DR1-MMA) CAS #119989-05-8, can be purchased from IBM Almaden Research Center, San Jose, Calif.; attn.: Dan Dawson, phone (408) 927-1617.]
15. D. Jungbauer, I. Teraoka, D. Y. Yoon, B. Reck, J. D. Swalen, R. Tweig, and C. G. Willson, "Second-order nonlinear optical properties and relaxation characteristics of poled linear epoxy polymers with tolane chromophores," J. Appl. Phys. **69,** 8011 (1991).
16. See, for example, M. Born and E. Wolf, *Principles of Optics* (Pergamon, New York, 1975), Sec. 14.2.
17. N. Bloembergen, *Nonlinear Optics* (Benjamin, New York, 1965), Chap. 4.
18. See Sec. 14.6 of Ref. 16.
19. D. Neher, A. Wolf, C. Bubeck, and G. Wegner, "Third-harmonic generation in polyphenylacetylene: exact determination of nonlinear optical susceptibilities in ultrathin films," Chem. Phys. Lett. **163,** 116 (1989).